BADI: A NOVEL BURNED AREA DETECTION INDEX FOR SENTINEL-2 IMAGERY USING GOOGLE EARTH ENGINE PLATFORM

H. Farhadi [1, *], H. Ebadi [1], A. Kiani [2]

[1] Faculty of Geodesy and Geomatics Engineering, K.N Toosi University of Technology, Tehran, Iran - hadifarhadi18@gmail.com, ebadi@kntu.ac.ir
[2] Faculty of Geodesy and Geomatics Engineering, Babol Noshirvani University of Technology, Babol, Iran - a.kiani@nit.ac.ir

Commission IV, WG IV/3

KEY WORDS: Fire, Remote Sensing, Spectral Index, Forest Fire, Burn Severity, Operational System.

ABSTRACT:

Forest fires are natural events that occur in numerous ecosystems worldwide and cause significant damage to human, ecological and socio-economic factors. It is also crucial to obtain useful information on the distribution and density of burned areas on large scale. An efficient way to map large regions is through remote sensing (RS). Nevertheless, the complex scenario and similar spectral signature of features in multispectral bands can lead to many false positives, making it difficult to extract the burned areas accurately. Multispectral data from Sentinel-2 satellite images allow the development of novel burned area indices, as more spectral data is recorded in the Red-Edge region. This research aims to develop a new burned area detection index (BADI) at 20 m spatial resolution in the google earth engine platform to detect the wildfire-affected areas in southwest of Iran using Sentinel-2 satellite imagery. The BADI spectral index has been specially designed to take benefit of the Sentinel-2 spectral bands and use a spectral combination of bands that are reasonable for post-fire burned regions detection. The final results indicated that the proposed index by applying a post-processing stage works well in the case of the study area to identify the burned areas. At the same time, it can satisfactorily suppress the complicated and irrelevant changes in the scene. Furthermore, the BADI index is rapid and can provide the burned areas map in near real-time. According to the Copernicus Emergency Management Service (EMS) reference data, maps of the burned areas were produced with a kappa coefficient of 0.92 and an overall accuracy of 92.15%, which demonstrated a good result in comparison to similar spectral indices.

1. INTRODUCTION

Vegetation fires are a common disaster in farms, and forests, wreaking havoc on human life and property, the environment, and wildlife. Every year, a high amount of forests and other regions are burned by fires in the entirety of the world, especially in Iran. Climate conditions, slopes, and vegetation areas all influence the direction, size, and power of wildfires (Thonicke et al., 2001). In order to manage an emergency, detailed products on the temporal and spatial distribution of burned areas are (BA) essential (Keane et al., 2001; Farhadi et al., 2022b). Because of complicated topography, extensive scenes, and poor weather conditions, traditional ground surveys can be costly and challenging. Analysis of multitemporal and multispectral imagery can quickly locate the BA using remote sensing (RS) (Tansey et al., 2008; Lizundia-Loiola et al., 2020; Farhadi et al., 2022b).

The extent of a wildfire can be determined both spatially and temporally using satellite images. Satellite sensors with multispectral capability such as Landsat-1 to 9, Sentinel-2 multispectral instruments (MSI), and MODIS provide reliable data in a short timeframe and medium spatial resolution (Giglio et al., 2018; Farhadi and Najafzadeh, 2021). Consequently, RS technology can provide valuable image data for burnt area monitoring. However, it is critical for fire suppression, and prevention of fire spread that fire-affected regions are mapped quickly and accurately after the fire (Farhadi et al., 2022b).

The Sentinel-2 optical satellite imagery has been used to create new spectral indices for BA detection recently (Filipponi, 2018). In recent studies, Sentinel-2 imagery's Red-Edge (RE) bands have been successfully applied to create a spectral index for assessing and detecting fire severity (Quintano et al., 2018; Liu et al., 2020). Following are several studies that used Sentinel-2 images to detect the BA.

Research on the severity of fires has become increasingly interesting in recent years. There are principally two kinds of spectral indicators that can be used to detect BA, including the vegetation index and the BA index (Patterson and Yool, 1998). The traditional method of BA detection is based on the composite burn index (CBI), which is a ground-based measure proposed by (Key, 2004). The CBI index remains the standard index used in field surveys and wildfire severity assessments by the United States Forest Service (USFS). The Normalized Burn Index (NBR) was first proposed by (García and Caselles, 1991) as an alternative to the Normalized Difference Vegetation Index (NDVI), where the red (R) band in the NDVI calculation formula is replaced by the short-wave infrared (SWIR) band. Further studies have demonstrated that the differential NBR (dNBR) index can better represent the spatial distribution of forest fire severity compared to the NBR index (TAN et al., 2016; Farhadi and Najafzadeh, 2021). Previous studies have shown that the NBR index is more sensitive to changes in chlorophyll and water content of vegetation, and have concluded that this index is the most practical RS approach for assessing fire severity. Despite the long relative success and

* Corresponding author

their common usage, NBR/dNBR spectral indices have some drawbacks in use. A first point to note is that the NBR/dNBR burned area detection index stays positively responsive to spectral variations other than those associated with wildfires (Roy et al., 2006). secondly, the connection between NBR/dNBR and fire severity becomes saturated for plots where the severity is high. This issue can also happen within field-observed indices when field observations are taken in a little range. This issue is hampering the NBR/dNBR index's ability to distinguish subtle differences between high severity plots. Thirdly, the association between NBR/dNBR and fire severity is environmentally-related, so field observations are needed to calibrate the NBR/dNBR (Alonso-Canas and Chuvieco, 2015). However, there is no consensus on which index performs agreeably in detecting the BA and considering wildfire severity, and under which situations it should be selected (Filipponi, 2018; Farhadi et al., 2022b).

Most studies to date on fire severity using RS images have been based on the SWIR, near-infrared (NIR), and red (R) spectral regions (Ruckstuhl and Norris, 2009). However, few investigations have associated the RE spectral band with wildfire severity. Filipponi, 2018 proposed the BA index for Sentinel-2 (BAIS2) based on the RE band of Sentinel-2 data (Filipponi, 2018). A study by Fernández-Manso et al. (2016) on fires in the Sierra de Gata in mid-western Spain in 2015 found that the RE band of Sentinel-2 data is very useful for estimating the extent of damage caused by fires and for monitoring post-fire reconstruction.

For the detection of BA, in addition to spectral indices, some other approaches have been used, including supervised classification using decision trees (DT), support vector machines (SVM), neural networks (NN) (Silva et al., 2005; Kontoes et al., 2009), and linear transformations (Patterson and Yool, 1998), spectral unmixing strategies (Lizundia-Loiola et al., 2020), and linear regression models (Koutsias and Karteris, 2000). In addition to being faster than other strategies, spectral indices-based methods can detect the BA without training samples (Chongo et al., 2007; Farhadi et al., 2022b). Despite this, the thresholds of the spectral indices need to be adjusted depending on the environmental attributes of the case study (Smith et al., 2007). Roteta et al. (2021) provided an application to map the BA using Sentinel-2 and Landsat satellite imagery on the GEE environment, based on supervised techniques. The results indicated that the method was efficient, with commission and omission errors of less than 12 percent. Therefore, due to the decrease in vegetation in satellite imagery before and after the fire, existing vegetation spectral indices can accurately determine differences in the BA. There is, however, the possibility that there are differences in spectral characteristics between different ground covers, such as soil, in some bands, such as SWIR and NIR.

In recent years, the wide availability of medium spatial resolution of optical imagery such as the Sentinel-2 satellite images equipped with dedicated spectral bands to collect data in the RE spectral region, which is one of the nicest radiation-based identifiers of chlorophyll and vegetation water amount (Curran et al., 1990), has paved the way for the development and application of novel spectral indicator to discriminate burnt severity. Recent investigations have proven successful in estimating the severity of burns using Sentinel-2 images by comparing satellite imagery taken before and after the fire (Fernández-Manso et al., 2016; Navarro et al., 2017; Mallinis et al., 2018; Quintano et al., 2018) and have demonstrated the usefulness of current RE spectral indicators for discriminating burned severity and Sentinel-2 MSI data for detecting the BA (Mallinis et al., 2018). This is indicative of the need for further analysis to produce a map of the BA using the Sentinel-2 images.

It is important to note that the RE and SWIR spectral bands are largely unaffected by aerosols, which makes them an excellent tool for monitoring vegetation as well as burned vegetation. in addition, the SWIR spectral bands contribute to an improved distinction between burnt and non-burned pixels (Giglio et al., 2018). SWIR reflectance is impacted by water absorption, which makes the SWIR spectral bands positively sensitive to the presence of water within vegetation. The reflectance of burned pixels will therefore be relatively high in the RE and SWIR bands, in contrast to the very low reflectance that is depicted in the NIR bands (Giglio et al., 2018). Moreover, when shifting from the NIR to SWIR spectral region, the reflectance differences between burned and non-burned pixels are significantly increased. The current study presents the novel BADI (Burned Area Detection Index) spectral index for the identification and mapping of the BA. The aforementioned index has been specially developed to take benefit of the Sentinel-2 spectral bands and use a spectral combination of bands that are reasonable for post-fire burned regions detection. The derived difference BADI (dBADI) index is based on the arithmetic difference between the before and after the fire BADI index estimate. BADI and dBADI were used to map fires that occurred in May 2020. The outcomes were compared with the reference indices and the Copernicus EMS outcomes. Ultimately, the development of a processor-based on BADI and dBADI indicators for the BA mapping is presented. The process of creating the map of the BA in the present work was carried out entirely using the web-based platform GEE. This platform may handle extensive processes in less time (Farhadi et al., 2022a). The GEE platform is used in other environmental scopes, including natural resource applications, agriculture, mapping and monitoring natural disasters (Kumar and Mutanga, 2018). Results of the mentioned effective index can be used in applications assessing fire hazards and estimating destruction due to it.

In general, the present study organization begins with an introduction to the study area and data sets in section 2. A detailed description of the proposed methodology is provided in the third section of the paper. Next, the outcomes are analysed qualitatively and quantitatively and compared with some of the recent studies. Ultimately, the main results are delivered in the conclusions section.

2. STUDY AREA AND DATA

2.1 Study Area

The fire event considered in this research occurred from 3 to 13 May 2020 in southwestern Iran and southwestern Fars province and 5 km from the town of Farashband (Figure 1). The study area is related to the Zone 39N of the UTM coordinate system. This place, located in Zagros Mountain, fire-damaged dozens of natural resources, including local flora and fauna. The Zagros Mountains on the western border of Iran, are dwelling of numerous individual kinds of fauna and flora. 40 % of herbs used for medicinal aims are found in this area. Nevertheless, drought and over-consumption of resources have harmed the region's woodlands, and nowadays forest fires are also threatening the region. Several local authorities reported that the wildfire caused severe damage to soil texture, biodiversity,

standard ecological functions, and losses among firefighter personnel. Also, elevation ranges from 750m to 1300m above sea level.

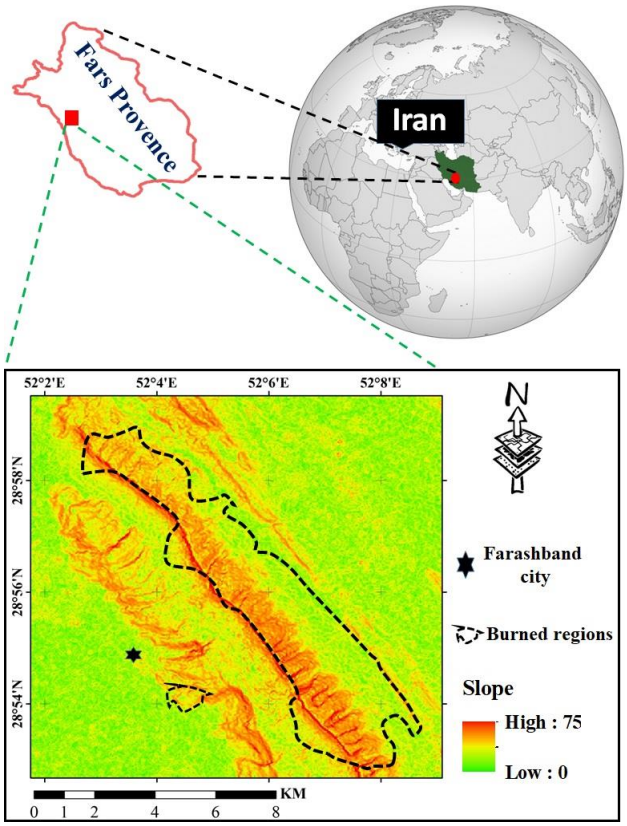

Figure 1. location of the study areas by the Slope model.

The reason for choosing this region as a study area is the happening of successive wildfires in that. In May 2020, a fire damaged 2055 hectares of forest land in the Farashband region, according to the Emergency Management Service (EMS). The current research utilised EMS wildfire maps with ID: EMSN079 as a test data map to assess the outcome of the proposed spectral index, as depicted in Figure 2. It is worth noting that the fire occurred on steep slopes.

2.2 Satellite Data

Cloud-free optical satellite images obtained by the Sentinel-2 satellite were used in the present study. There are two satellites in the Sentinel-2 constellation and the revisit time is five days. The Sentinel-2A satellite was launched in June 2015, while Sentinel-2B was launched in July 2016. Satellite imagery from Sentinel-2 provides 13 spectral bands, covering the visible, NIR, and short-wave infrared (SWIR) regions with spatial resolutions from 10 meters to 60 meters. The spectral and spatial information for the Sentinel-2 satellite can be found in Table 1.

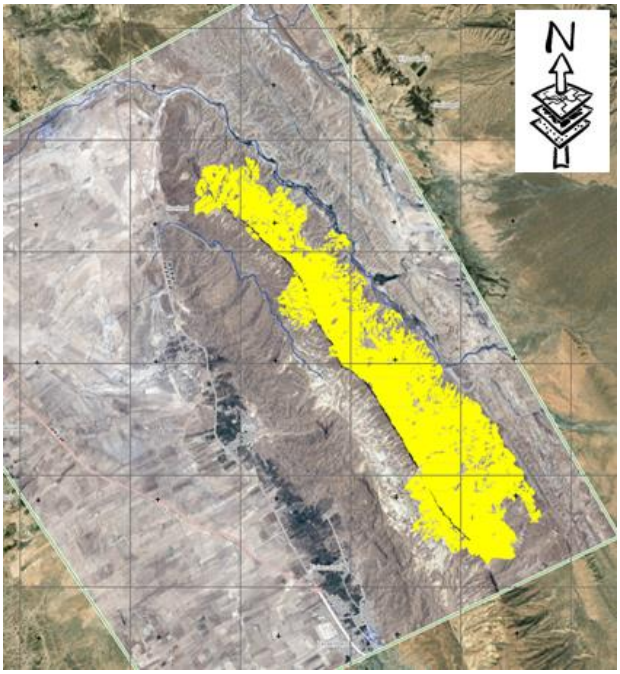

Figure 2. The EMS map to evaluate the result.

In the current research, the Level-1C products available at GEE (Dataset ID: "COPERNICUS /S2_SR") were used. In the first phase, the Sentinel-2 dataset was mosaicked in the GEE web-based platform to fully cover the study region. Subsequently, mosaicked images were atmospherically restored to the reflectance of the L-2A bottom of atmosphere (BOA) using the Sen2cor (Farhadi et al., 2022b), and resampled to a spatial resolution of 20 m. Ultimately, atmospherically corrected images were used for the calculation of the spectral index. The used Sentinel-2A image scenes related to before and after the fire is shown in Figure 3.

Name	Resolution	Wavelength	Description
B1	60 meters	443.9 nm	Aerosols
B2		496.6 nm	Blue
B3	10 meters	560 nm	Green
B4		664.5 nm	Red
B5		703.9 nm	Red EDG 1
B6	20 meters	740.2 nm	Red EDG 2
B7		782.5 nm	Red EDG 3
B8	10 meters	835.1 nm	NIR
B8A	20 meters	864.8 nm	Red EDG 4
B9	60 meters	945 nm	Water Vapor
B10		1373.5 nm	Cirrus
B11	20 meters	1613.7 nm	SWIR-1
B12		2202.4 nm	SWIR-2

Table 1. Characteristics of the Sentinel-2A MSI bands.

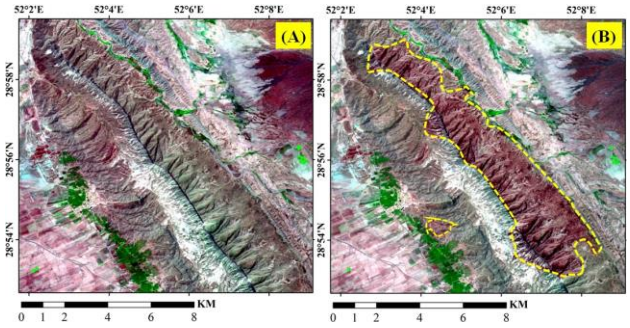

Figure 3. Sentinel-2 images, pre-fire (A), and post-fire (B).

3. METHODOLOGY

The current research provides a robust spectral index for the accurate and rapid detection of BA using Sentinel-2 imagery in the GEE environment. After importing the Sentinel-2 imagery related to pre-fire and post-fire and applying the required preprocessing stages in the GEE platform, the novel Sentinel-2 burned area detection index (BADI) was used to create a map of the primary burned regions (PBR). In the following phase, to enhance the BA identification accuracy, NDWI (normalised difference water index) and NDVI indices were used to mask the pixels associated with permanent water bodies and live vegetation. To compute the optimal threshold of the index automatically, we used the Otsu histogram thresholding technique (Otsu, 1979). Ultimately, the final burned regions (FBR) are obtained by subtracting the pre and post-fire water and vegetation pixels from the PBR. The procedures for carrying out the proposed index are shown in Figure 4. The details are provided below.

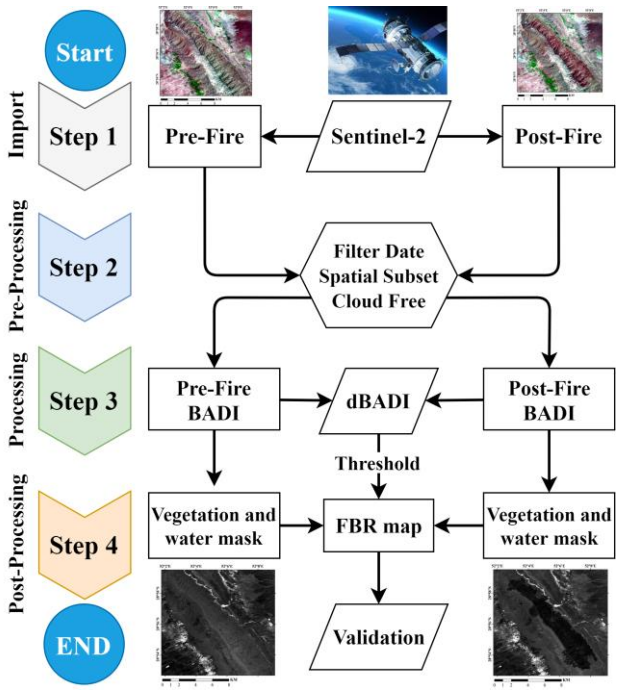

Figure 4. Flowchart of the novel BADI index for burned area detection.

3.1 Proposed Burned Area Detection Index (BADI)

Different spectral signatures from the visible to the SWIR range have different trends for a given phenomenon before and after the fire periods. Because of the high importance of SWIR, NIR, and R bands in spectral indices, the ratio of mentioned bands was used in most previous studies. Figure 5 shows a scatter plot of the vegetation pixel values in the different spectral bands, related to the time before (Figure 5a) and after the fire (Figure 5b). As shown in Figure 5a, the vegetation pixel values in the SWIR-1 band do not overlap with other bands. On the other hand, the RE1 band has a significant reflective distance compared to the SWIR-1 band. Although the SWIR-2 band before the fire contains the same information as the other bands, in the post-fire time both the SWIR-1 and SWIR-2 bands have provided useful information to better distinguish the BA. Therefore, using visible, RE, NIR and SWIR bands can provide useful information in identifying the BA.

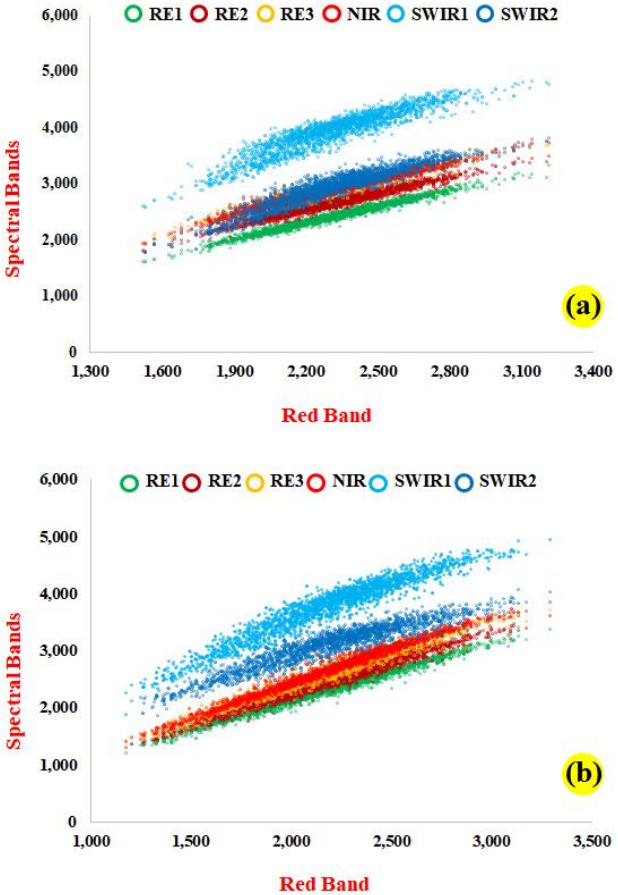

Figure 5. Scatter plot for vegetated areas in the different spectral bands; pre-fire (a), post-fire (b).

The novel BADI spectral index for burned area detection can be estimated using Equations 1-3. To identify wildfire-impacted areas, mentioned index utilizes the spectral components of the NIR and RE bands.

$$F1 = \left(\frac{(B12 + B11) - (B8 + B8A)}{\sqrt{(B12 + B11) + (B8 + B8A)}} \right) \quad (1)$$

$$F2 = \left(2 - \sqrt{\frac{B6 \times B7 \times (B8 + B8A)}{B4 + B5}} \right) \quad (2)$$

$$BADI = F1 \times F2 \quad (3)$$

In Equation (1-2), B4, B5, B6, B7, B8, B8A, B11, and B12 are the corresponding bands of Sentinel-2 images and BADI represents the novel burned area index in before and after images.The dBADI index between the two images at different periods is computed by subtracting the BADI indices before and after the fire (Equation 4). The PBR map is generated after the automatically Otsu thresholding technique has been applied to the dBADI index.

$$dBADI = BADI_{\text{Pre}} - BADI_{Post} \quad (4)$$

3.2 FBR Map by Water and Vegetation Mask

The BADI index for burnt area detection is sensitive to vegetation and water classes due to the spectral bands used. Since the properties of vegetation and water land cover classes are different pre and post-fire, the areas containing vegetation and water are identified as burnt pixels. To solve this problem, misidentified pixels should be recognized over time (before, during and after the wildfire) and removed from the PBR map result. To distinguish water pixels from other land cover classes like vegetation, bare soil, and burned pixels, the useful NDWI index was used in this study. In the index mentioned above, positive values $(NDWI >= 0)$ were categorized as water pixels, while negative values $(NDWI < 0)$, were determined as non-water pixels (McFeeters, 1996; Farhadi et al., 2022b). The NDWI spectral index for water area detection can be estimated using Equation 5; where B3 and B8 are the corresponding bands of the sentinel-2 images.

$$NDWI = (B3 - B8) / (B3 + B8) \quad (5)$$

Another class that complicates the identification of burnt areas is healthy vegetation, which must be masked from PBR map results. In the current research, NDVI was used to detect the vegetated pixels, which can be calculated using Equation 6. The NDVI index value ranges between -1 and +1, which NDVI greater than 0.2 being decided as vegetation. B4 and B8 are the corresponding bands of the sentinel-2 images (Tucker, 1979; Farhadi et al., 2022a).

$$NDVI = (B4 - B8) / (B4 + B8) \quad (6)$$

Possible water (NDWI) and vegetation pixels (NDVI) are removed from the PBR map recognized as primarily burnt regions to obtain the FBR map. Therefore, an FBR map can be calculated for each image pair (before and after the wildfire) according to Equation 7.

$$FBR = PBR - (NDVI + NDWI) \quad (7)$$

3.3 Evaluation of the Results

An evaluation of the proposed BADI index was conducted based on the EMS reference map. According to a visual interpretation of the extant EMS map, sampling was carried out in two sets of burnt and unburnt points or polygons. A random sample of 200 pixels was assigned to each class (burned or unburned) for testing. In addition, in the current study, the confusion matrix (CM) of the map of the burnt area was used for the statistical evaluation of accuracy. As shown in Table 2, four measures of accuracy (Equations 9-12) obtained from the CM were used to evaluate the outcomes: producer accuracy (PA %), user accuracy (UA%), overall accuracy (OA%), and kappa coefficient (KC). Where, Xii: number of observed samples in row i and column i, Xjj: number of observed samples in row j and column j, c: number of land cover class, N: total number of samples, r: number of rows, and Xi+, X+j: the marginal totals for row i and column j, respectively. In addition, a comparison between the performance of the suggested index and spectral indices used in burnt area detection (Table 3) was conducted by the separability index (SI). SI can be calculated for each image pair (before and after the wildfire) according to Equation 8.

$$SI = \frac{|M_b - M_{ub}|}{(S_b + S_{ub})} \quad (8)$$

Where M_b and S_b depict the average and standard deviation of the samples from the burnt regions and M_{ub} and S_{ub} for the average and standard deviation of the samples from the non-burnt areas. Therefore, $SI > 1$ depicts fine separation, whereas values of $SI < 1$ representing lousy separation(Mallinis et al., 2018; Farhadi et al., 2022b).

To compare the BADI index with the reference spectral indicators used for mapping the BA, BAIS2, NBR, normalized difference SWIR (NDSWIR), and mid-infrared bispectral index (MIRBI) were calculated according to Table 3; where, B4, B8, B11 and B2 are the corresponding bands of the sentinel-2 images.

Index	Formula
OA	$OA = \frac{\sum_{i=1}^{c} X_{ii}}{N}$ (9)
KC	$KC = \frac{N \sum_{i=1}^{r} X_{ii} - \sum_{i=1}^{r} X_{i+} X_{+j}}{N^2 - \sum_{i=1}^{r} X_{i+} X_{+j}}$ (10)
UA	$UA_j\,\% = \frac{X_{jj}}{\sum_{i=1}^{c} X_{ij}} \times 100$ (11)
PA	$PA_i\,\% = \frac{X_{ii}}{\sum_{j=1}^{c} X_{ij}} \times 100$ (12)

Table 2. Accuracy evaluation benchmarks from CM.

4. RESULTS AND DISCUSSIONS

This section presents the results of the suggested spectral index for mapping the BA. Then, the outcomes are compared qualitatively and quantitatively with various spectral indicators. (shown in Table 3).

Name	Formula
BAIS2	$\left(1 - \sqrt{\frac{B6 \times B7 \times B8A}{B4}}\right) \times \left(\frac{B12 - B8A}{\sqrt{B12 + B8A}} + 1\right)$, (13)

NBR	$(B8 - B12) / (B8 + B12)$,	(14)
NDSWIR	$(B8 - B11) / (B8 + B11)$,	(15)
MIRBI	$10 \times B12 - 9.8 \times B11 + 2$,	(16)

Table 3. Popular sentinel-2 burnt detection spectral indices.

4.1 Qualitative and Visual Evaluation

A visual comparison was performed between the suggested BADI index and popular spectral indices using different spectral difference images. Figure 6 illustrates the comparison of the BADI index with the four spectral indices, including BAIS2 (Filipponi, 2018), NBR, NDSWIR (Gerard et al., 2003), and MIRBI (Trigg and Flasse, 2001) indices, difference and their binary maps results in the study area.

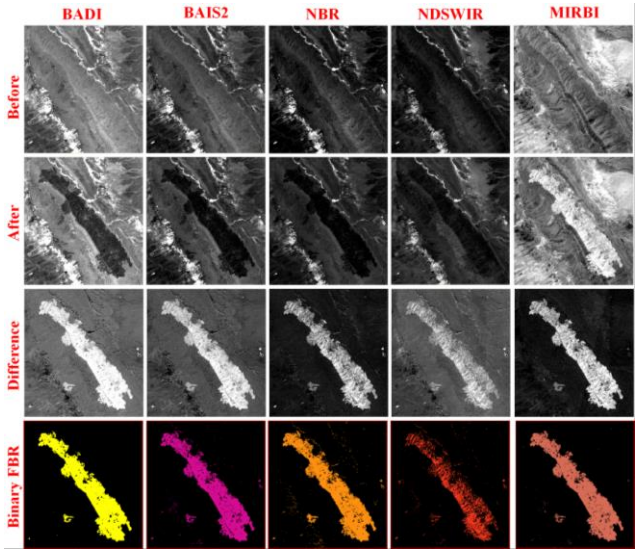

Figure 6. Burned area detection indices related to the study area; pre-fire (First row), post-fire (Second row), difference maps (Third row), and binary maps (End row).

As shown in Figure 6, the BADI spectral index clearly distinguishes burnt regions from other land cover classes. Consequently, the suggested index can accurately monitor the Spatio-temporal characteristics of the BA. This method can also predict the direction of fire spread by analyzing two or more images, which can be helpful for spatial modelling of the BA and wildfire hazard assessment. As the visual interpretation results in Figure 6 show, the BADI index is not affected by interfering classes such as soil or bare land, vegetated pixels, built-up area and water due to post-processing strategies. Therefore, the suggested index obtained significant accuracy in visual assessment.

The result of the spatial distribution of the burnt regions from the BADI index (FBR) and the same scope spectral indices for the BA detection, including the BAIS2, NBR, MIRBI and NDSWIR indices are shown in Figure 7 for part of the study areas. According to Figure 7, in the study region, other classes such as water, soil, or bare land, vegetated pixels and built-up areas are also recognized as burnt pixels in the binary map of wildfire spectral indices in the literature. In contrast, the binary map of the BADI index has no false classes and most pixels are associated with BA. Compared to existing burned detection spectral indices, the proposed index performed well visually in regions where no wildfires have happened.

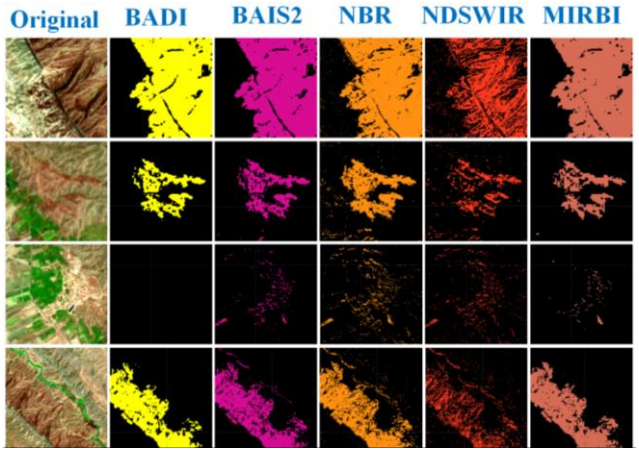

Figure 7. Portions of the original image (B12, B8, B4) and their local-scale binary maps in the study area. Columns 2-5 show the different binary maps extracted from the spectral indices.

4.2 Quantitatively Accuracy Evaluation

The statistical accuracy results of the binary map obtained by different spectral indices for two scenarios (burned and unburned classes) are illustrated in Table 4. The most elevated values for the individually binary maps are depicted in bold.

Index	Classes	OA	KC	UA	PA
BADI	burnt	**92.15**	**0.92**	91.12	**92.47**
	unburnt			**91.63**	91.85
BAIS2	burnt	87.23	0.85	88.45	89.12
	unburnt			89.41	90.15
NBR	burnt	85.19	0.78	88.35	87.36
	unburnt			87.14	88.44
MIRBI	burnt	88.14	0.86	91.19	90.41
	unburnt			91.43	92.25
NDSWIR	burnt	81.32	0.78	84.32	84.42
	unburnt			85.21	84.69

Table 4. The accuracy assessment of the wildfire detection.

Based on Table 4, the OA of the proposed index (BADI) in the study area is 92.12%. In contrast, the OA for BAIS2, NBR, MIRBI and NDSWIR indices are 87.23, 85.19, 88.14 and 81.32%, respectively. Based on the OA, the suggested index gives better accurate outcomes than the same spectral indices. The maximum and minimum OA values were 92.15% and 81.32% concerning the BADI and NDSWIR indices, respectively. Additionally, the UA of the proposed binary index map for burnt and unburnt regions in the study area were 91.12 and 91.63%, respectively. Moreover, the PA amounts of the proposed index binary map for burnt and unburnt pixels were 92.47 and 91.85%, respectively. The KC of the BADI index in the study area is 0.92. In contrast, the KC for the BAIS2, NBR, MIRBI and NDSWIR indicators are 0.85, 0.78, 0.86 and 0.78, respectively. In comparison with the other indices, the proposed index provides more accurate results based on the KC criterion. The SI calculation statistics are shown in Table 5. The most elevated values for the SI are depicted in bold.

BADI	BAIS2	NBR	MIRBI	NDSWIR
2.19	1.9	1.2	2.05	1.05
dBADI	dBAIS2	dNBR	dMIRBI	dNDSWIR
3.89	3.56	2.4	3.7	1.8

Table 5. SI results by burnt and unburnt regions for suggested and popular wildfire spectral indices.

5. CONCLUSIONS

Fires are a natural danger that sometimes occurs in farms and forests causing irreversible damage to possessions and human life, wildlife, and environmental variables. Due to the spectral variation within each class, mapping burnt regions over a large area is challenging. In this research, a novel spectral index (namely BADI index) was specifically developed to fully take benefit of the Sentinel-2 spectral bands (R, NIR, SWIR, and RE bands) characteristics on the GEE for rapid and robust burned areas detection. The main goal of this research was to detect and map the burned areas using the proposed BADI spectral index in the GEE environment accurately and automatically. In the first step, the Sentinel-2 data was acquired and pre-processed in the GEE environment. In the second step, the BA map was extracted using the BADI spectral index and the automatic Otsu thresholding method. In the next step, water and vegetation classes were removed from the PBR map to create the FBR map. The ultimate accuracy was then assessed according to the EMS product. The final map of BA had a kappa coefficient of 0.92 and an overall accuracy of 92.15%. The proposed BADI index was very accurate in comparison to some popular and reference spectral indicators like BAIS2, NBR, MIRBI and NDSWIR. Moreover, the results of the suggested spectral index can be employed as training data for fire risk management or prediction. More specifically, it is more beneficial to evaluate the BA from the point of view of temporal change detection and efficiently implement unsupervised change detection without depending on training data. The high accuracy of our burnt area mapping index shows that spectral indices using RS imagery and a GEE platform can be successfully applied to remote sensing applications requiring little processing time. The result of the current research shows that automatic detection of BA can be accomplished with great accuracy at the GEE by deriving the BADI index from Sentinel-2 images. According to the research findings, through the accurate mapping of permanent water and vegetation cover, and removing them from the burned areas map, a significant improvement in the accuracy of the final BA map was achieved. Furthermore, our study confirmed that the GEE environment is an effective tool that facilitates the immediate production of BA maps.

The clouds caused by the fire and the dense smoke make it challenging to visit the BA in the optical satellite data. In such cases, Sentinel-1 SAR images can be a good option due to their long wavelength and the passage of waves through thick smoke. In future investigations, integrating or harmonising different passive (Optical) and active (Radar) RS sensors could improve burned area detection outcomes.

REFERENCES

Alonso-Canas, I., Chuvieco, E., 2015. Global burned area mapping from ENVISAT-MERIS and MODIS active fire data. Remote Sensing of Environment, 163, 140-152. doi.org/10.1016/j.rse.2015.03.011.

Chongo, D., Nagasawa, R., Ould Cherif Ahmed, A., Perveen, M.F., 2007. Fire monitoring in savanna ecosystems using MODIS data: a case study of Kruger National Park, South Africa. Landscape and Ecological Engineering, 3, 79-88. doi.org/10.1007/s11355-007-0020-5.

Curran, P.J., Dungan, J.L., Gholz, H.L., 1990. Exploring the relationship between reflectance red edge and chlorophyll content in slash pine. Tree physiology, 7, 33-48. doi.org/10.1093/treephys/7.1-2-3-4.33.

Farhadi, H., Managhebi, T., Ebadi, H., 2022a. Buildings extraction in urban areas based on the radar and optical time series data using Google Earth Engine. Scientific-Research Quarterly of Geographical Data (SEPEHR), 30, 43-63. 10.22131/SEPEHR.2022.251053.

Farhadi, H., Mokhtarzade, M., Ebadi, H., Beirami, B.A., 2022b. Rapid and automatic burned area detection using sentinel-2 time-series images in google earth engine cloud platform: a case study over the Andika and Behbahan Regions, Iran. Environmental Monitoring and Assessment, 194, 1-19. doi.org/10.1007/s10661-022-10045-4.

Farhadi, H., Najafzadeh, M., 2021. Flood risk mapping by remote sensing data and random forest technique. Water, 13, 3115. doi.org/10.3390/w13213115.

Fernández-Manso, A., Fernández-Manso, O., Quintano, C., 2016. SENTINEL-2A red-edge spectral indices suitability for discriminating burn severity. International journal of applied earth observation and geoinformation, 50, 170-175. doi.org/10.1016/j.jag.2016.03.005.

Filipponi, F., 2018. BAIS2: Burned area index for Sentinel-2. Multidisciplinary digital publishing institute proceedings, 2, 364. doi.org/10.3390/ecrs-2-05177.

García, M.L., Caselles, V., 1991. Mapping burns and natural reforestation using Thematic Mapper data. Geocarto International, 6, 31-37. doi.org/10.1080/10106049109354290.

Gerard, F., Plummer, S., Wadsworth, R., Sanfeliu, A.F., Iliffe, L., Balzter, H., Wyatt, B., 2003. Forest fire scar detection in the boreal forest with multitemporal SPOT-VEGETATION data. IEEE Transactions on Geoscience and Remote Sensing, 41, 2575-2585. doi.org/10.1109/TGRS.2003.819190.

Giglio, L., Boschetti, L., Roy, D.P., Humber, M.L., Justice, C.O., 2018. The Collection 6 MODIS burned area mapping algorithm and product. Remote sensing of environment, 217, 72-85. doi.org/10.1016/j.rse.2018.08.005.

Keane, R.E., Burgan, R., van Wagtendonk, J., 2001. Mapping wildland fuels for fire management across multiple scales: Integrating remote sensing, GIS, and biophysical modeling. International Journal of Wildland Fire, 10, 301-319. doi.org/10.1071/WF01028.

Key, C.H., 2004. Landscape assessment: ground measure of severity, the composite burn index; and remote sensing of severity, the normalized burn ratio. FIREMON: Fire effects monitoring and inventory system. USGS.

Kontoes, C., Poilvé, H., Florsch, G., Keramitsoglou, I., Paralikidis, S., 2009. A comparative analysis of a fixed thresholding vs. a classification tree approach for operational burn scar detection and mapping. International Journal of Applied Earth Observation and Geoinformation, 11, 299-316. doi.org/10.1016/j.jag.2009.04.001.

Koutsias, N., Karteris, M., 2000. Burned area mapping using logistic regression modeling of a single post-fire Landsat-5 Thematic Mapper image. International Journal of Remote Sensing, 21, 673-687. doi.org/10.1080/014311600210506.

Kumar, L., Mutanga, O., 2018. Google Earth Engine applications since inception: Usage, trends, and potential. Remote Sensing, 10, 1509. doi.org/10.3390/rs10101509.

Liu, S., Zheng, Y., Dalponte, M., Tong, X., 2020. A novel fire index-based burned area change detection approach using Landsat-8 OLI data. European journal of remote sensing, 53, 104-112. doi.org/10.1080/22797254.2020.1738900.

Lizundia-Loiola, J., Otón, G., Ramo, R., Chuvieco, E., 2020. A spatio-temporal active-fire clustering approach for global burned area mapping at 250 m from MODIS data. Remote Sensing, of Environment 236, 111493. doi.org/10.1016/j.rse.2019.111493.

Mallinis, G., Mitsopoulos, I., Chrysafi, I., 2018. Evaluating and comparing Sentinel 2A and Landsat-8 Operational Land Imager (OLI) spectral indices for estimating fire severity in a Mediterranean pine ecosystem of Greece. GIScience & Remote Sensing, 55,1-18. doi.org/10.1080/15481603.2017.1354803.

McFeeters, S.K., 1996. The use of the Normalized Difference Water Index (NDWI) in the delineation of open water features. International journal of remote sensing, 17, 1425-1432. doi.org/10.1080/01431169608948714.

Navarro, G., Caballero, I., Silva, G., Parra, P.-C., Vázquez, Á., Caldeira, R., 2017. Evaluation of forest fire on Madeira Island using Sentinel-2A MSI imagery. International Journal of Applied Earth Observation and Geoinformation, 58, 97-106. doi.org/10.1016/j.jag.2017.02.003.

Otsu, N., 1979. A threshold selection method from gray-level histograms. IEEE transactions on systems, man, andcybernetics, 9, 62-66. doi.org/10.1109/TSMC.1979.4310076.

Patterson, M.W., Yool, S.R., 1998. Mapping fire-induced vegetation mortality using Landsat Thematic Mapper data: A comparison of linear transformation techniques. Remote Sensing of Environment, 65, 132-142. doi.org/10.1016/S0034-4257(98)00018-2.

Quintano, C., Fernández-Manso, A., Fernández-Manso, O., 2018. Combination of Landsat and Sentinel-2 MSI data for initial assessing of burn severity. International journal of applied earth observation and geoinformation, 64, 221-225. doi.org/10.1016/j.jag.2017.09.014.

Roteta, E., Bastarrika, A., Franquesa, M., Chuvieco, E., 2021. Landsat and Sentinel-2 based burned area mapping tools in google earth engine. Remote Sensing, 13, 816. doi.org/10.3390/rs13040816.

Roy, D.P., Boschetti, L., Trigg, S.N., 2006. Remote sensing of fire severity: assessing the performance of the normalized burn ratio. IEEE Geoscience and Remote Sensing Letters, 3, 112-116. doi.org/10.1109/LGRS.2005.858485.

Ruckstuhl, C., Norris, J.R., 2009. How do aerosol histories affect solar “dimming” and “brightening” over Europe?: IPCC-AR4 models versus observations. Journal of Geophysical Research: Atmospheres, 114. doi.org/10.1029/2008JD011066.

Silva, J.M., Sá, A.C., Pereira, J.M., 2005. Comparison of burned area estimates derived from SPOT-VEGETATION and Landsat ETM+ data in Africa: Influence of spatial pattern and vegetation type. Remote sensing of environment, 96, 188-201. doi.org/10.1016/j.rse.2005.02.004.

Smith, A., Drake, N., Wooster, M., Hudak, A., Holden, Z., Gibbons, C., 2007. Production of Landsat ETM+ reference imagery of burned areas within Southern African savannahs: comparison of methods and application to MODIS. International Journal of Remote Sensing, 28, 2753-2775. doi.org/10.1080/01431160600954704.

TAN, L., ZENG, Y., ZHENG, Z., 2016. An adaptability analysis of remote sensing indices in evaluating fire severity. Remote Sensing for Land & Resources, 84-90. doi.org/10.6046/gtzyyg.2016.02.14.

Tansey, K., Grégoire, J.M., Defourny, P., Leigh, R., Pekel, J.F., Van Bogaert, E., Bartholomé, E., 2008. A new, global, multi-annual (2000–2007) burnt area product at 1 km resolution. Geophysical Research Letters, 35. doi.org/10.1029/2007GL031567.

Thonicke, K., Venevsky, S., Sitch, S., Cramer, W., 2001. The role of fire disturbance for global vegetation dynamics: coupling fire into a Dynamic Global Vegetation Model. Global Ecology and Biogeography, 10, 661-677. doi.org/10.1046/j.1466-822X.2001.00175.x.

Trigg, S., Flasse, S., 2001. An evaluation of different bi-spectral spaces for discriminating burned shrub-savannah. International Journal of Remote Sensing, 22, 2641-2647. doi.org/10.1080/01431160110053185.

Tucker, C.J., 1979. Red and photographic infrared linear combinations for monitoring vegetation. Remote sensing of Environment, 8, 127-150. doi.org/10.1016/00344257(79)90013-0.